This article was downloaded by: [Chongqing University]
On: 14 February 2014, At: 13:26
Publisher: Taylor & Francis
Informa Ltd Registered in England and Wales Registered Number: 1072954 Registered office: Mortimer House, 37-41 Mortimer Street, London W1T 3JH, UK

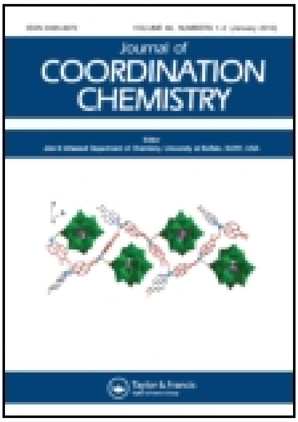

Journal of Coordination Chemistry
Publication details, including instructions for authors and subscription information:
http://www.tandfonline.com/loi/gcoo20

Syntheses, structures, and characterizations of three Ag(I) complexes constructed by length-modulated pyrazole-based ligands

Guang-Feng Hou[a], Ying-Hui Yu[ab], Xue Wang[a], Jin-Sheng Gao[ab], Bo Wen[a], Xiao-Dan Wang[a] & Peng-Fei Yan[a]

[a] Engineering Research Center of Pesticide of Heilongjiang University, Heilongjiang University, Harbin, China

[b] School of Chemistry and Materials Science, Heilongjiang University, Harbin, China

Accepted author version posted online: 05 Sep 2013.Published online: 22 Oct 2013.

To cite this article: Guang-Feng Hou, Ying-Hui Yu, Xue Wang, Jin-Sheng Gao, Bo Wen, Xiao-Dan Wang & Peng-Fei Yan (2013) Syntheses, structures, and characterizations of three Ag(I) complexes constructed by length-modulated pyrazole-based ligands, Journal of Coordination Chemistry, 66:19, 3402-3411, DOI: 10.1080/00958972.2013.840774

To link to this article: http://dx.doi.org/10.1080/00958972.2013.840774

PLEASE SCROLL DOWN FOR ARTICLE

Taylor & Francis makes every effort to ensure the accuracy of all the information (the “Content”) contained in the publications on our platform. However, Taylor & Francis, our agents, and our licensors make no representations or warranties whatsoever as to the accuracy, completeness, or suitability for any purpose of the Content. Any opinions and views expressed in this publication are the opinions and views of the authors, and are not the views of or endorsed by Taylor & Francis. The accuracy of the Content should not be relied upon and should be independently verified with primary sources of information. Taylor and Francis shall not be liable for any losses, actions, claims, proceedings, demands, costs, expenses, damages, and other liabilities whatsoever or howsoever caused arising directly or indirectly in connection with, in relation to or arising out of the use of the Content.

This article may be used for research, teaching, and private study purposes. Any substantial or systematic reproduction, redistribution, reselling, loan, sub-licensing, systematic supply, or distribution in any form to anyone is expressly forbidden. Terms &

Journal of Coordination Chemistry, 2013
Vol. 66, No. 19, 3402–3411, http://dx.doi.org/10.1080/00958972.2013.840774

Syntheses, structures, and characterizations of three Ag(I) complexes constructed by length-modulated pyrazole-based ligands

GUANG-FENG HOU†, YING-HUI YU†‡, XUE WANG†, JIN-SHENG GAO*†‡,
BO WEN†, XIAO-DAN WANG† and PENG-FEI YAN†

†Engineering Research Center of Pesticide of Heilongjiang University, Heilongjiang University,
Harbin, China
‡School of Chemistry and Materials Science, Heilongjiang University, Harbin, China

(*Received 15 September 2012; accepted 5 August 2013*)

Three coordination complexes with N-donor ligands, $Ag_2(L1)_{1.5}(NO_3)_2$ (**1**), $Ag_3(L2)_2(NO_3)_3$ (**2**), and $Ag(L1)_2NO_3$ (**3**) {**L1** = 1,4-bis(pyrazole-1-ylmethyl)benzene, **L2** = 4,4′-bis(pyrazole-1-ylmethyl) biphenyl}, have been synthesized and structurally characterized by elemental analysis, IR spectroscopy, TGA, and X-ray single crystal diffraction. Complex **1** shows a 3-D *fsh*-3,4-$P2_1/c$ structure with brevity code $\{8^3\}^2\{8^5{\cdot}10\}$. Complex **2** has a 3-D framework with a 2-D layer penetrated by an infinite 1-D zigzag chain. Complex **3** exhibits a (4,4)-net racemizing layer structure with nitrate anions filling the cavity. The results indicate that **L1** and **L2** can adopt varied conformations in formation of the complexes, and the length of the ligands plays a key role in configuring and directing the corresponding structure of the complexes.

Keywords: Ag(I) complex; Crystal structure; Length-modulated ligand

1. Introduction

Design and construction of metal-organic coordination frameworks are of interest due to their structural diversity and potential applications in heterogeneous catalysis, molecular recognition, magnetism, gas storage, ion exchange, nonlinear optics, and electrical conductivity [1–4]. N-containing ligands, such as imidazole and pyrazole derivatives, play an important role because of their good coordination and ability to transmit electronic effects [5–8]. One example is 1,4-bis(imidazol-1-ylmethyl)benzene (bix) consisting of a rigid phenyl linking two coordinated groups *via* flexible methylene sp^3-carbons. Such structural feature endows semi-rigidity to bix, which could construct discrete metallomacrocycles, 1-D infinite chains, 2-D polyrotaxane networks, and 3-D frameworks when reacting with metal ions [9–13]. Previous research also shows that bix is particularly useful in formation of interpenetrating networks [14], catenanes [15], and polyrotaxanes [16]. As a sequel to our continuing efforts in exploring the influence of ligands with different coordination sites

---

*Corresponding author. Email: gaojins@hlju.edu.cn on the structures of coordination polymers [17], we change imidazole groups in bix to pyrazole groups obtaining 1,4-bis(pyrazol-1-ylmethy)benzene (**L1**) to tune the coordination direction and conformation of the ligand, which may lead to new coordination complexes. Thus far, a series of polyoxometalates (POMs) supported **L1** and Cu^I complexes were reported, showing 0D to 3-D structure and bearing surface photovoltaic and electrochemical properties [18]. We also synthesized 4,4′-bis(pyrazole-1-ylmethyl)biphenyl (**L2**) to investigate the effect of ligand length on the structures of their coordination complexes (scheme 1).

These two pyrazole-containing ligands have flexibility and rigidity in coordinating as the building blocks, which makes it possible to take *trans*- or *cis*-conformations. Furthermore, different spacers give different molecular length, which may fulfill the expectation of obtaining different crystal configurations. However, formation of inorganic–organic supramolecules is influenced by factors such as the geometry of metal ions, the nature of ligands, counterions, the ratio of metal salt and ligand, and solvent system or templates. Thus, understanding how these considerations affect metal coordination and crystal packing is at the forefront of controlling coordination supramolecular arrays.

Herein, we report the crystal structures of three complexes obtained from the reaction of $AgNO_3$ with **L1** and **L2**: $\{[Ag_2(L1)_{1.5}(NO_3)_2]\}_n$ (**1**) is a 3-D framework; $\{[Ag_3(L2)_2(NO_3)_3]\}_n$ (**2**) shows a penetrated supramolecular structure consisting of 1D coordination motifs interpenetrating a 2-D layer; by changing the molar ratio of ligand and Ag^I, we obtained $\{[Ag(L1)_2(NO_3)]\}_n$ (**3**) which is an enantiomeric layer structure. All complexes were characterized by single-crystal X-ray diffraction analysis, elemental analysis, IR analysis, and thermal gravimetric analysis (TGA).

2. Experimental

2.1. *Materials and methods*

Commercial chemicals were of reagent grade and used as received. Elemental analyses were performed on a CARLO ERBA 1106 analyzer. IR spectra were recorded on a Bruker IFS

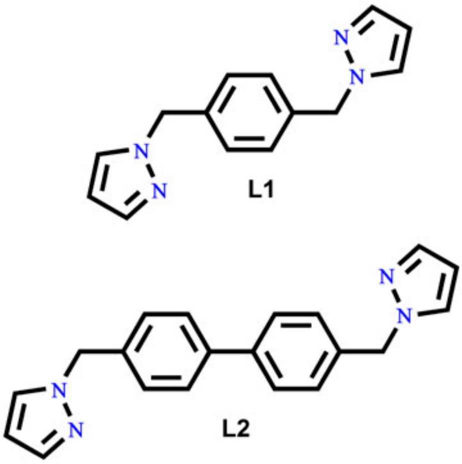

Scheme 1. Schematic representation of 1,4-bis(pyrazole-1-ylmethyl)benzene (**L1**) and 4,4′-bis(pyrazole-1-ylmethyl) biphenyl (**L2**).

66v FT-IR spectrometer equipped with a DGTS detector (32 scans) by using KBr pellets. ^{1}H NMR spectra were performed on a Bruker AV 300 MHz spectrometer. Thermogravimetric measurements were done on a Perkin–Elmer TGA 7 analyzer.

2.2. *Preparation of L1 and L2*

L1 and **L2** were synthesized using an improved method described elsewhere [19]. A mixture of pyrazole (9.0 g, 130 mM) and NaOH (5.5 g, 130 mM) in DMSO (40 mL) was stirred at 50 °C for 1 h and 1,4-bis(chloro)benzene (10.50 g, 60 mM) for **L1** or 4,4′-bis (chloro)bibenzene (15.06 g, 60 mM) for **L2** in DMSO (60 mL) was added. The mixture was cooled to room temperature after being stirred at 60 °C for 24 h and poured into 200 mL water. White solid that formed immediately was isolated by filtration and then dried in air (**L1**: 10.8 g, 75% yield; **L2**: 11.8 g, 82% yield). Elemental analysis: Calcd for **L1**-$C_{14}H_{14}N_4$: C, 70.57; H, 5.92; N, 23.51%. Found: C, 70.41; H, 5.79; N, 23.80%. IR (KBr, cm^{-1}): 3116 (m), 2934 (w), 2857 (w), 1812 (w), 1759 (w), 1516 (s), 1451 (s), 1424 (s), 1398 (s), 1357 (s), 1284 (s), 1229 (s), 1092 (s), 1050 (s), 958 (s), 807 (s), 762 (s), 744 (s), 615 (m), 483 (s). ^{1}H NMR ($CDCl_3$): 5.29 (2H, s, CH_2), 6.27 (1H, t), 7.17 (2H, d), 7.36 (1H, d), 7.53 (1H, d). Elemental analysis: Calcd for **L2**-$C_{20}H_{18}N_4$: C, 76.41; H, 5.77; N, 17.82%. Found: C, 76.78; H, 5.50; N, 17.72%. IR (KBr, cm^{-1}): 3113 (w), 2933 (w), 1638 (w), 1515 (m), 1441 (m), 1397 (s), 1281 (m), 1094 (m), 1054 (m), 970 (m), 837 (m), 802 (m), 758 (s), 750 (s), 623 (m). ^{1}H NMR ($CDCl_3$): 5.37 (2H, s, CH_2), 6.31 (1H, t), 7.27 (2H, d), 7.43 (1H, d), 7.52 (2H, d), 7.57 (1H, d).

2.3. *Syntheses of 1–3*

2.3.1. Synthesis of $[Ag_2(L1)_{1.5}(NO_3)_2]$ (1). An aqueous solution (5 mL) of $AgNO_3$ (17.0 mg, 0.1 mM) was added slowly with constant stirring to an acetonitrile solution (5 mL) of **L1** (23.8 mg, 0.1 mM) to give a clear solution. The mixture was heated to 50 °C and stirred for 1 h. After filtration, colorless blocks suitable for X-ray diffraction were obtained in 37% yield by slow evaporation at room temperature for several days. Elemental analysis: Calcd for $C_{21}H_{21}N_8Ag_2O_6$: C, 36.18; H, 3.04; N, 16.07%. Found: C, 36.15; H, 3.13; N, 16.14%. IR (KBr, cm^{-1}): 3434 (s), 3109 (w), 1634 (m), 1517 (m), 1384 (s), 1340 (s), 1162 (m), 1059 (m), 1019 (w), 974 (m), 829 (w), 775 (s), 616 (m).

2.3.2. Synthesis of $[Ag_3(L2)_2(NO_3)_3]$ (2). Complex **2** was obtained in 47% yield by procedure similar to the synthesis of **1** except that **L2** (31.4 mg, 0.1 mM) was used instead of **L1**. Elemental analysis: Calcd for $C_{40}H_{36}Ag_3N_{11}O_9$: C, 42.20; H, 3.19; N, 13.53%. Found: C, 42.11; H, 3.29; N, 13.54%. IR (KBr, cm^{-1}): 3435 (s), 3109 (w), 1635 (m), 1517 (m), 1385 (s), 1340 (s), 1162 (w), 1102 (m), 1019 (w), 974 (m), 829 (w), 775 (s), 616 (m).

2.3.3. Synthesis of $[Ag(L1)_2(NO_3)]$ (3). Complex **3** was obtained in 42% yield by procedure similar to the synthesis of **1** except that more **L1** (47.6 mg, 0.2 mM) was used. Elemental analysis: Calcd for $C_{28}H_{28}AgN_9O_3$: C, 42.20; H, 3.19; N, 13.53%. Found: C, 42.11; H, 3.09; N, 13.51%. IR (KBr, cm^{-1}): 3428 (s), 3109 (w), 1628 (m), 1517 (m), 1385 (s), 1340 (s), 1163 (w), 1102 (m), 1059 (w), 977 (w), 762 (m), 617 (m).

2.4. *X-ray Crystallography*

Single-crystal X-ray diffraction data for **1–3** were collected on a Rigaku R-AXIS RAPID imaging plate diffractometer with graphite-monochromated Mo K_α ($\lambda = 0.71073$ Å) radiation at 291 K. Empirical absorption corrections based on equivalent reflections were applied. The structures of **1–3** were solved by direct methods and refined by full-matrix least-squares on F^2 using SHELXS-97 crystallographic software package [20]. All non-hydrogen atoms were refined anisotropically. Hydrogens bound to carbons were placed in calculated positions and treated as riding on their parent with C−H = 0.93 Å (aromatic) or 0.97 Å (methylene), and with U_{iso} (H) = 1.2 U_{eq} (C). The nitrates in **2** are disordered, with one nitrate disordered over two positions with occupancies of 0.5 for each position, while two oxygens in the other nitrate are also disordered over two positions with occupancies of 0.5 for each position. One nitrate in **3** is disordered, with two O disordered over two positions and refined occupancies of 0.55(2), 0.45(2), 0.48(1) and 0.52(1) for O1, O1′, O2 and O2′, respectively. Crystal parameters, data collections and refinement results for **1–3** are summarized in table 1. Crystallographic data have been deposited to the Cambridge Crystallographic Data Centre with the deposition numbers CCDC 735295, 738533, and 746818 for 1–3, respectively.

3. Results and discussion

3.1. *Crystal structure descriptions*

To investigate the influence of bridging ligands with different lengths on the formation of supramolecular architectures, **L1** with phenyl linker and **L2** with biphenyl linker are selected to react with $AgNO_3$.

Table 1. Crystal data and structure refinements for **1–3**.

	1	**2**	**3**
Empirical formula	$C_{21}H_{21}N_8Ag_2O_6$	$C_{40}H_{36}Ag_3N_{11}O_9$	$C_{28}H_{28}AgN_9O_3$
Fw	697.20	1138.41	646.46
Crystal system	Monoclinic	Triclinic	Monoclinic
Space group	$P2_1/c$	$P\bar{1}$	Cc
a (Å)	10.035(2)	8.3484(17)	14.749(3)
b (Å)	6.481(3)	9.5230(19)	14.332(3)
c (Å)	16.114(5)	14.903(3)	13.346(3)
α (°)	90	90.22(3)	90
β (°)	113.84(2)	104.12(3)	97.06(3)
γ (°)	90	112.79(3)	90
V (Å^3)	2437.7(10)	1031.7(4)	2799.9(10)
Z	4	1	4
D_{Calcd} (g cm^{-3})	1.900	1.832	1.534
μ (mm^{-1})	1.662	1.480	0.768
$F(000)$	1380	566	1320
Collected/unique	23,147/5551	8199/3612	13,376/6062
R(int)	0.0283	0.0296	0.0209
GOF on F^2	1.026	1.090	1.016
$R_1{}^a[I > 2\sigma(I)]$	0.0312	0.0501	0.0315
$wR_2{}^b[I > \sigma(I)]$	0.0755	0.1554	0.0810
$R_1{}^a$(all)	0.0392	0.0690	0.0373
$wR_2{}^b$ (all)	0.0791	0.1751	0.0839

${}^aR_1 = (\Sigma||F_o| - |F_c|)/\Sigma|F_o|$.
${}^b wR_2 = [\Sigma w(F_o{}^2 - F_c{}^2)^2/\Sigma w(F_o{}^2)^2]^{1/2}$.

3.1.1. Complex 1. Single-crystal X-ray diffraction analysis shows that the asymmetric unit of 1 consists of two Ag^I cations, two NO_3^-, one full and one half **L1**. As shown in figure 1a, there are three crystallographically unique Ag^I cations, with different coordination spheres. Ag1 is a T-shaped coordination environment connected with two N from two pyrazoles and one O from nitrate. Ag–N bond distances are 2.156(2)–2.164(2) Å, Ag1–O bond distance is 2.720(3) Å and the N–Ag–N coordination angle is 172.29(9) (table 2). However, Ag2 is five-coordinate in a tetragonal pyramid, connected with one N from **L1** and four O from two nitrates; the Ag2–O bond distances are 2.337(3) –2.646(3) Å and the Ag2–N bond distance is 2.210(3) Å (table 2). Two Ag2 ions are connected by two nitrates to form a dimer with Ag2 Ag2^I distance of 4.04 Å. **L1** links Ag1 to Ag2 with *cis-* and Ag1 to Ag1 with

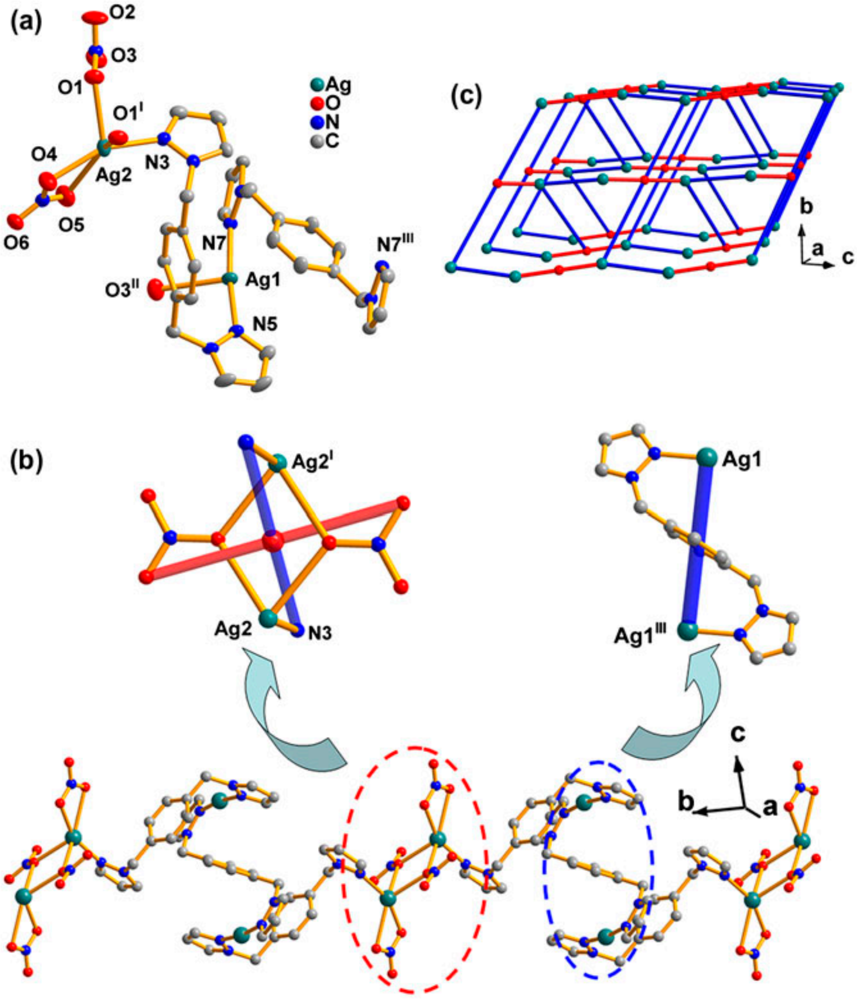

Figure 1. (a) Molecule structure of 1 with the ellipsoids drawn at the 50% probability level, where hydrogens are omitted for clarity; (b) 1D helical chain structure of **1**; (c) Schematic illustration of 3D *fsh*-3,4-$P2_1/c$ structure with the brevity code $\{8^3\}^2\{8^5.10\}$. Symmetry codes: (I) $1-x$, $-1-y$, $1-z$; (II) $-x$, $0.5+y$, $0.5-z$; (III) $-x$, $-y$, $1-z$.

trans-conformation constructing a 1-D zigzag chain (figure 1b). A 3-D framework is constructed by Ag1 Ag2 (3.245(1) Å) and Ag O (2.720 (3) Å) weak interactions between adjacent chains. Topological analysis indicates a 3-D fsh-3,4-$P2_1/c$ structure with brevity code $\{8^3\}^2\{8^5\cdot 10\}$ when the Ag2O2 dimer is reduced to a four connected node (figure 1c). Ag–Ag or Ag–O weak interactions play an important role in the packing structure, which have been well documented [21].

3.1.2. Complex 2.

To evaluate the influence of the length of ligand on the product structure, **L2** with longer spacer is used to synthesize **2**. Single-crystal X-ray diffraction analysis reveals that **2** crystallizes in the triclinic system with $P\bar{1}$ space group. The asymmetric unit of **2** consists of two crystallographically independent Ag^{I} cations, two NO_3^-, and two half **L2** (figure 2a). In **2**, Ag1 is in a disordered coordination environment with Ag–O bond distance from 2.400(12) to 2.467(12) Å and the Ag–N bond distance of 2.207(5) Å (table 2). These bond distances are consistent with reported values of Ag–N-containing complexes [22]. Two adjacent Ag1 are linked by weak Ag1–O1 (2.799(1) Å) coordination interaction to form dimers with Ag·Ag distance of 6.090(2) Å. These dimers are linked by other nitrates and *trans*-conformation **L2** to form a 2D square grid with large cavities of approximately 13.07 × 8.35 Å^2 (figure 2b). However, Ag2 is two coordinate by two *trans*-conformation **L2** [N(3)#2–Ag(2)–N(3) 180.00°] to build up a zigzag chain. Interestingly, these

Table 2. Selected bond lengths and angles for **1–3**.

Complex **1**			
Ag(1)–N(5)	2.156(2)	Ag(1)–N(7)	2.164(2)
Ag(1)–O(3)^{II}	2.720(3)	Ag(2)–N(3)	2.210(3)
Ag(2)–O(4)	2.337(3)	Ag(2)–O(1)	2.529(2)
Ag(2)–O(1)^{I}	2.545(2)	Ag(2)–O(5)	2.646(3)
Ag(1)–Ag(2)^{II}	3.245(1)		
N(5)–Ag(1)–N(7)	172.29(9)	N(5)–Ag(1)–O(3)^{II}	97.07(9)
N(7)–Ag(1)–O(3)^{II}	90.48(9)	N(3)–Ag(2)–O(4)	156.81(10)
N(3)–Ag(2)–O(1)	92.60(9)	O(4)–Ag(2)–O(1)	110.55(9)
N(3)–Ag(2)–O(1)^{I}	95.15(9)	O(1)–Ag(2)–O(1)^{I}	74.45(8)
N(3)–Ag(2)–O(5)	113.31(9)	O(4)–Ag(2)–O(5)	49.87(8)
O(1)–Ag(2)–O(5)	130.95(10)	O(1)#2–Ag(2)–O(5)	137.87(8)
Symmetry codes: I: $-x+1$, $-y-1$, $-z+1$; II: $-x$, $y+1/2$, $-z+1/2$			
Complex **2**			
Ag(1)–N(1)	2.207(5)	Ag(1)–O(1)	2.400(12)
Ag(1)–O(7)	2.467(12)	Ag(1)–O(6)^{III}	2.544(16)
Ag(1)–O(2)	2.763(10)	Ag(2)–N(3)	2.129(4)
N(1)–Ag(1)–O(1)	143.2(2)	N(1)–Ag(1)–O(7)	124.9(3)
O(1)–Ag(1)–O(7)	83.0(4)	N(1)–Ag(1)–O(6)^{III}	114.3(4)
O(1)–Ag(1)–O(6)^{III}	94.7(5)	O(7)–Ag(1)–O(6)^{III}	74.8(4)
N(1)–Ag(1)–O(2)	116.2(3)	O(1)–Ag(1)–O(2)	46.0(4)
O(7)–Ag(1)–O(2)	118.8(4)	O(6) #1–Ag(1)–O(2)	78.2(4)
N(3)–Ag(1)–N(3)^{III}	180.00		
Symmetry codes: I: $-x+2$, $-y+2$, $-z+1$; II: $-x$, $-y+1$, $-z+1$; III: $-x+2$, $-y+1$, $-z$; IV: $-x+1$, $-y+2$, $-z+1$			
Complex **3**			
Ag(1)–N(1)	2.304(3)	Ag(1)–N(5)	2.338(3)
Ag(1)–N(8)^{II}	2.344(3)	Ag(1)–N(4)^{I}	2.414(3)
N(1)–Ag(1)–N(5)	116.02(10)	N(1)–Ag(1)–N(8)^{II}	121.75(10)
N(1)–Ag(1)–N(4)^{I}	96.61(11)	N(5)–Ag(1)–N(8)^{II}	100.69(11)
N(5)–Ag(1)–N(4)^{I}	112.09(10)	N(8)^{II}–Ag(1)–N(4)^{I}	109.97(11)
Symmetry codes: I: $x+1/2$, $y-1/2$, z; II: $x+1/2$, $y+1/2$, z			

zigzag chains penetrate the above-mentioned 2-D square layers to form a 1-D-penetrated 2-D supramolecular framework (figure 2c).

3.1.3. Complex 3. To evaluate the effect of reactant molar ratio in the construction of the supramolecular architectures, complex **3** is obtained when the ligand/metal ratio increased from 1 to 2. Single-crystal X-ray diffraction analysis reveals that **3** crystallizes in the monoclinic system with *Cc* space group. The asymmetric unit of **3** consists of one Ag^{I}, one uncoordinated disordered NO_3^-, and two **L1**. As shown in figure 3a, each Ag^{I} is four coordinated in tetrahedral geometry defined by four N from four **L1** ligands with Ag–N bond distance from 2.304(3) to 2.414(3) Å (table 2). In **3**, two crystallographically independent **L1** both exhibiting *cis*-conformations bridge Ag^{I} to form an undulating 2D (4,4)-net with each cavity size of 10.283(2) Å × 10.283(2) Å (figure 3b). The uncoordinated nitrates fill cavities, stabilized by hydrogen bonds (table S1).

Adjacent planes are enantiomers caused by different coordination directions (figure 3c). Similar phenomena have been found in $[Mn(bna)(DMF)_2(H_2O)_2]_n \cdot n(DMF)$ [23] and $\{[Cd(L6)_{0.5}(BIE)(H_2O)] \cdot H_2O\}$ [24] [H_2bna = 2,2′-dihydroxyl-[1,1′]-binaphthalene3,3′-dicarboxylate acid; H_4L_6 = 4,4′-oxidiphthalic acid; BIE = 2,2′-bis(1H-imdazolyl)ether]. We believe that the sp^3-carbon confers a rigid ligand certain flexibility, which probably favors the

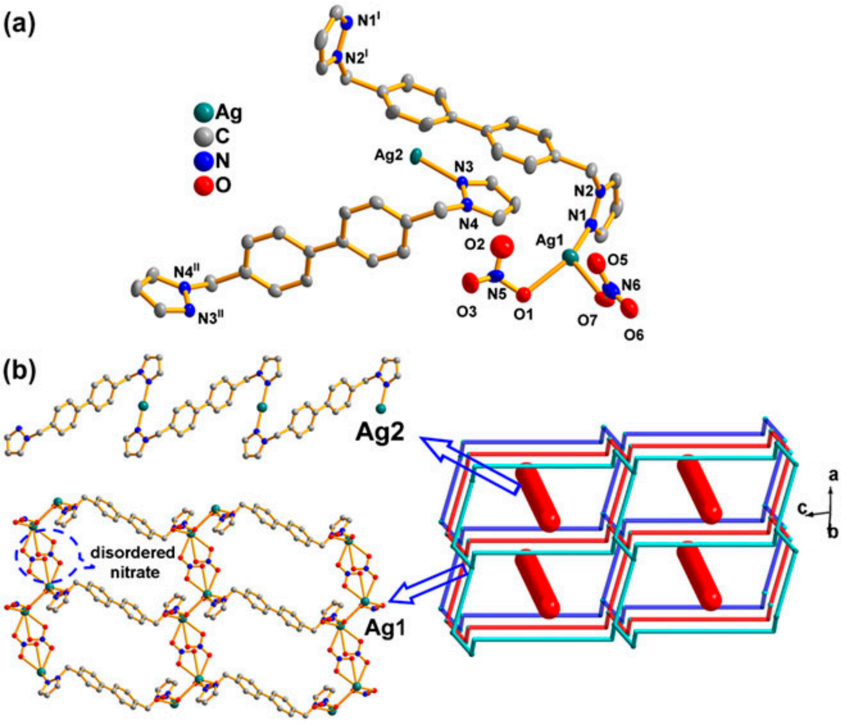

Figure 2. (a) Molecule structure of **2** with the ellipsoids drawn at the 50% probability level. (b) 2D network of **2**. (c) View of a topology of **2**. Symmetry codes: (I) 2 – *x*, 2 – *y*, 1 – *z*; (II) –*x*, 1 – *y*, 1 – *z*.

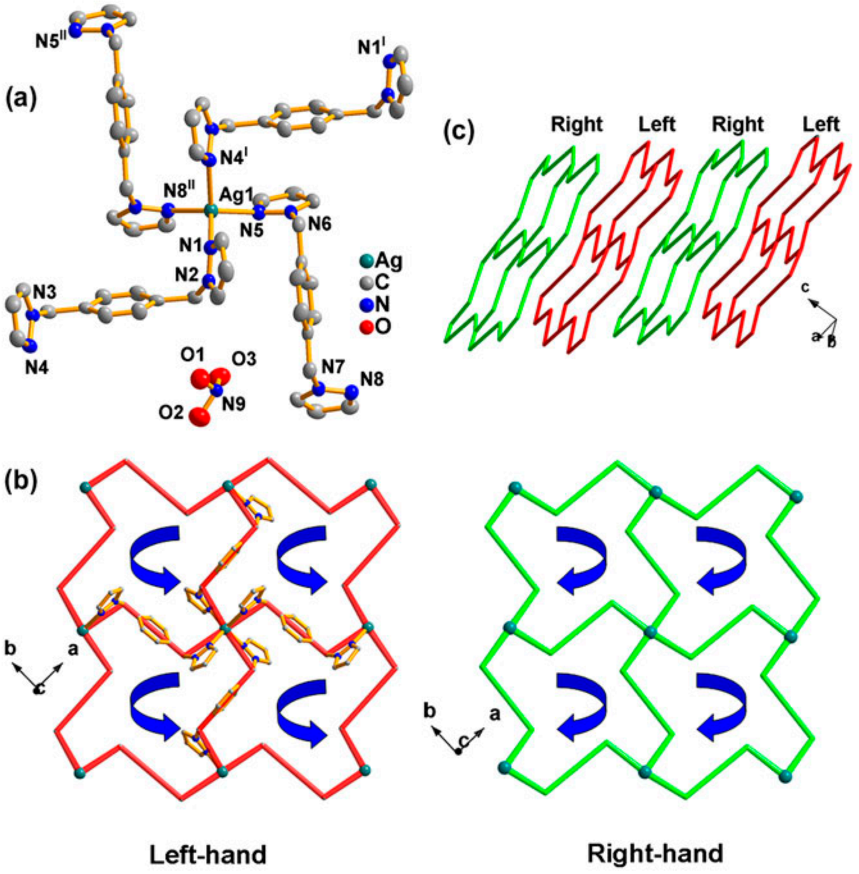

Figure 3. (a) Coordination environment of Ag(I) in **3** with the ellipsoids drawn at the 50% probability level; disordered O atoms of nitrates are omitted for clarity. (b) 2D chiral cavity of **3**. (c) Schematic illustration of stacking structure of **3**. Symmetry codes: (I) $0.5 + x, -0.5 + y, z$; (II) $0.5 + x, 0.5 + y, z$.

construction of the chiral layer structure. Moreover, distorted coordination sites of N in pyrazole also increased the possibility of such chiral structure formation.

3.2. *Thermal properties*

TGA were carried out to examine the thermal stabilities of **1–3**. The samples were heated in flowing N_2 with a heating rate of 10 °C min^{-1}. The TGA curves indicate that **1** is stable to 203 °C, from which point the framework begins to collapse. The observed final mass remnant of 27.21% is ascribed to deposition of Ag_2O (Calcd: 32.09%). However, **2** and **3** show the weight loss from beginning, caused by loss of adsorbed water. Complexes **2** and **3** are stable to 220 and 240 °C, respectively, from which point the frameworks begin to collapse, and the residues may be ascribed to Ag_2O.

4. Conclusions

Three inorganic–organic complexes **1–3** have been synthesized and characterized, and their structural relationships with the reaction conditions were investigated. Results reveal that the ligand and reactant molar ratio have effects on controlling the structures of coordination complexes: (i) Complexes **1** and **2** were synthesized at the same conditions except that ligands with different lengths are used. Complex **1** exhibits a 3D *fsh*-3,4-$P2_1/c$ structure constructed by **L1**, while **2** shows a 1D-penetrated 2D structure owning to the large cavity formed by longer **L2**. (ii) Complex **1** was synthesized in 1 : 1 M ratio (metal : ligand), in which Ag is coordinated with two **L1**; in contrast to that, **3** was synthesized in 1 : 2 M ratio, in which Ag is coordinated with four **L1**. These results could provide promising access to the rational design and synthesis of metal-organic coordination polymers with specific structures.

Acknowledgments

We acknowledge the support of the Natural Science Foundation of Heilongjiang Province (B201108), Scientific Research Fund of Heilongjiang Provincial Education Department (12531512), and Heilongjiang University.

References

[1] (a) H.H. Wu, Q.H. Gong, D.H. Olson, J. Li. *Chem. Rev.*, **112**, 836 (2012); (b) O.R. Evans, W.B. Lin. *Acc. Chem. Res.*, **35**, 511 (2002); (c) B.L. Chen, S.C. Xiang, G.D. Qian. *Acc. Chem. Res.*, **43**, 1115 (2010); (d) J.P. Zhang, Y.B. Zhang, J.B. Lin, X.M. Chen. *Chem. Rev.*, **112**, 1001 (2012).

[2] (a) M. Eddaoudi, J. Kim, N. Rosi, D. Vodak, J. Wachter, M. O'Keeffe, O.M. Yaghi. *Science*, **295**, 469 (2002); (b) J.S. Seo, D. Whang, H. Lee, S.I. Jun, J. Oh, Y.J. Jeon, K. Kim. *Nature*, **404**, 982 (2000).

[3] (a) E. Haldoupis, S. Nair, D.S. Sholl. *J. Am. Chem. Soc.*, **134**, 4313 (2012); (b) A.C. Mckinlay, R.E. Morris, P. Horcajada, G. Férey, R. Gref, P. Couvreur, C. Serre. *Angew. Chem., Int. Ed.*, **49**, 6260 (2010).

[4] (a) J.L.C. Rowsell, A.R. Millward, K.S. Park, O.M. Yaghi. *J. Am. Chem. Soc.*, **126**, 5666 (2004); (b) Y.Y. Jia, H.J. Li, Q.Q. Guo, B. Zhao, Y. Zhao, H.W. Hou, Y.T. Fan. *Eur. J. Inorg. Chem.*, **2012**, 3047 (2012).

[5] (a) Z. Su, M. Chen, T.A. Okamura, M.S. Chen, S.S. Chen, W.Y. Sun. *Inorg. Chem.*, **50**, 985 (2011); (b) L. Lou, P. Wang, G.C. Xu, Q. Liu, K. Chen, Y. Lu, Y. Zhao, W.Y. Sun. *Cryst. Growth Des.*, **12**, 2634 (2012).

[6] (a) R.Q. Zou, C.S. Liu, Z. Huang, T.L. Hu, X.H. Bu. *Cryst. Growth Des.*, **6**, 99 (2006); (b) C.S. Liu, X.S. Shi, J.J. Wang, X.H. Bu. *Cryst. Growth Des.*, **6**, 656 (2006).

[7] (a) C.Z. Li, X.R. Huang, Y.H. Chen. *J. Coord. Chem.*, **65**, 3699 (2012); (b) Y.H. Wen, Y.Y. Chen, H.L. Wen, X.L. Xie, L. Wang. *J. Coord. Chem.*, **65**, 2780 (2012).

[8] (a) C.H. Jiao, C.H. He, J.C. Geng, G.H. Cui. *J. Coord. Chem.*, **65**, 2852 (2012); (b) J.S. Solanki, T.R. Thapak, A. Bhardwaj, U.N. Tripathi. *J. Coord. Chem.*, **65**, 369 (2012).

[9] (a) A.C. Kathalikkattil, K.K. Bisht, N. Aliaga-Alcalde, E. Suresh. *Cryst. Growth Des.*, **11**, 1631 (2011); (b) L. Carlucci, G. Ciani, D.M. Proserpio. *Cryst. Growth Des.*, **5**, 37 (2005); (c) B.K. Tripuramallu, P. Manna, S.N. Reddy, S.K. Das. *Cryst. Growth Des.*, **12**, 777 (2012); (d) K.H. He, W.C. Song, Y.W. Li, Y.Q. Chen, X.H. Bu. *Cryst. Growth Des.*, **12**, 1064 (2012).

[10] (a) J. Yang, J.F. Ma, Y.Y. Liu, J.C. Ma, S.R. Batten. *Cryst. Growth Des.*, **8**, 4383 (2008); (b) Y.Y. Xu, Y.Y. Xing, X.Y. Duan, Y.Z. Li, H.Z. Zhu, Q.J. Meng. *Cryst. Eng. Commun.* **12**, 567 (2010).

[11] (a) X.L. Sun, W.C. Song, S.Q. Zang, C.X. Du, H.W. Hou, T.C.W. Mark. *Chem. Commun.*, **48**, 2113 (2012); (b) L. Carlucci, G. Ciani, D.M. Proserpio. *Chem. Commun.*, **40**, 380 (2004).

[12] (a) H. Wu, H.Y. Liu, Y.Y. Liu, J. Yang, B. Liu, J.F. Ma. *Chem. Commun.*, **47**, 1818 (2011); (b) J. Yang, J.F. Ma, S.R. Batten, Z.M. Su. *Chem. Commun.*, **44**, 2233 (2008).

[13] (a) J.X. Meng, Y. Lu, Y.G. Li, H. Fu, E.B. Wang. *Cryst. Eng. Commun.* **13**, 2479 (2011); (b) P.P. Zhang, J. Peng, J.Q. Sha, A.X. Tian, H.J. Pang, Y. Chen, M. Zhu. *Cryst. Eng. Commun.* **11**, 902 (2009); (c) J.X. Meng, Y. Lu, Y.G. Li, H. Fu, E.B. Wang. *Cryst. Growth Des.*, **9**, 4116 (2009).

[14] (a) L.L. Wen, Y.Z. Li, Z.D. Lu, J.G. Lin, C.Y. Duan, Q.J. Meng. *Cryst. Growth Des.*, **6**, 530 (2006); (b) L. Carlucci, G. Ciani, S. Maggini, D.M. Proserpio. *Cryst. Growth Des.*, **8**, 162 (2008).

[15] B.F. Hoskins, R. Robson, D.A. Slizys. *J. Am. Chem. Soc.*, **119**, 2952 (1997).
[16] J. Yang, J.F. Ma, S.R. Batten. *Chem. Commun.*, **48**, 7899 (2012).
[17] Y. Liu, P.F. Yan, Y.H. Yu, G.F. Hou, J.S. Gao, J.Y. Lu. *Cryst Growth Des.*, **10**, 1559 (2010).
[18] (a) G.F. Hou, L.H. Bi, B. Li, L.X. Wu. *Inorg. Chem.*, **49**, 6474 (2010); (b) G.F. Hou, L.H. Bi, B. Li, B. Wang, L.X. Wu. *CrystEngComm*, **13**, 3526 (2011).
[19] B.F. Hoskins, R. Robson, D.A. Slizys. *J. Am. Chem. Soc.*, **119**, 2952 (1997).
[20] G.M. Sheldrick. *Acta Cryst.*, **A64**, 112 (2008).
[21] (a) X.W. Wu, X.Y. Wang, Q.L. Li, J.P. Ma, Y.B. Dong. *J. Coord. Chem.*, **65**, 3299 (2012); (b) N.C. Kasuga, R. Yamamoto, A. Hara, A. Amano, K. Nomiya. *Inorg. Chim. Acta*, **359**, 4412 (2006).
[22] (a) F. Marandi, A. Marandi, M. Ghadermazi, H. Krautscheid, M. Rafiee. *J. Coord. Chem.*, **65**, 1882 (2012); (b) Y.J. Liang, X.J. Meng, F.P. Huang, J.J. Guo, Y.M. Jiang. *J. Coord. Chem.*, **64**, 3751 (2011); (c) J.A. Zhao, J.Y. Hu, Y. Bai, S.F. Chen, S.S. Li. *J. Coord. Chem.*, **65**, 3216 (2012).
[23] Q. Gao, F.L. Jiang, M.Y. Wu, Y.G. Huang, W. Wei, M.C. Hong. *Cryst. Growth Des.*, **10**, 184 (2010).
[24] L.P. Zhang, J.F. Ma, J. Yang, Y.Y. Liu, G.H. Wei. *Cryst. Growth Des.*, **9**, 4660 (2009).